

Investigation of Empirical and Analytical Methods Accuracy for Surface Settlement Prediction in Train Tunnel Excavation Projects

**Ali Maroof¹, Danial Mohammadzadeh S.^{2,3},
Nader Karballaezadeh^{4*}, Kiarash Sabourian Bajgiran³,
Amir Mosavi^{5*} and Imre Felde⁵**

¹ Faculty of Civil, Water, and Environmental, Shahid Beheshti University, 1983969411 Tehran, Iran; M_marooof@sbu.ac.ir

² University of Applied Science and Technology, Education Center of Mashhad Worker's House, 9188945449 Mashhad, Iran; Danial.Mohammadzadehshadmehri@mail.um.ac.ir

³ Department of Civil Engineering, Mashhad Branch, Islamic Azad University, 9187147578 Mashhad, Iran; D.mohammadzadeh.sh@mshdiau.ac.ir

⁴ Faculty of Civil Engineering, Science and Research Branch of Islamic Azad University, 1477893855 Tehran, Iran; N.karballaezadeh@Shahroodut.ac.ir

⁵ John von Neumann Faculty of Informatics, Óbuda University, Bécsi út 96/b, H-1034 Budapest, Hungary; Amir.mosavi@uni-obuda.hu, Felde@uni-obuda.hu

* Corresponding Authors

Abstract: Ground deformation, due to tunneling, is one of the most significant challenges in tunnel design in soft ground along with, the predicting the related effects of tunneling on nearby structures. One of the methods of predicting ground settlement in tunneling projects, is to use analytical and numerical methods. By measuring the amount of settlement with accurate instruments and back-analysis of behavioral measurement data, in addition to estimating the state of settlement of the ground and surrounding structures, it is possible to determine the geotechnical parameters of the soil and structure in the design of upcoming sections and future designs. In this study, an attempt has been made to verify the measured settlements caused by digging the tunnel of an urban train line, by using back analysis. For this purpose, comparisons with predictions obtained from empirical and analytical methods and the Geotechnical Engineering Finite Element Analysis software (PLAXIS) was used. The results show that often, the empirical methods obtain values more than the measured values, for ground settlement.

Keywords: Tunnel excavation; surface settlement; back analysis; PLAXIS; civil engineering; infrastructures; transportation; mobility

1 Introduction

Displacements that occur in the ground, which are the result of tunneling activities in urban environments, is one of the most important challenges in digging shallow tunnels in soft ground that usually exists in urban areas is the problem of land settlement and its impact on the nearby urban structures and facilities [1]. Further, ground-borne vibrations from railway or tramway tracks can cause damage to nearby urban structures and facilities [2-6]. Reliable forecasting of the aforementioned displacements, to assess possible human-financial losses and consider protective measures to reduce the above risks, are very useful. The effects on nearby structures such as existing tunnels, deep foundations, and so on, depend on the extent of the surface settlement profile and its amount. The effects of this change of location on the surface and buried structures and their servicing should be checked and settlement should be prevented if necessary. Displacements resulting from tunnel excavation in the soft ground can be predicted by various methods, including experimental methods based on field measurements [7-10], empirical and semi-empirical methods [11-13], numerical models [1, 14, 15], and physical models [16]. In these relationships, parameters such as the tunnel properties and its depth, the ground conditions, and the amount of volume reduction or convergence caused by tunnel digging are effective. The amount of ground settlement, its direction, and location within the tunnel depend on geotechnical conditions, static stresses in the ground and loads on the surface, underground water conditions, tunnel excavation method, and the type of tunnel lining. The recorded data provides the possibility of comparing analytical methods with monitoring data and calibrating and validating the numerical methods [1].

One of the best methods for estimating the ground displacements in upcoming sections is the back analysis and numerical modeling of the monitoring values measured in similar conditions. Back analysis can approximate the cross-section of settlements with the Gaussian distribution curve [7], by fitting the monitoring data with the Gaussian curve parameters. In the present research, the observed settlements in the northern part of Mashhad city urban train line 2, are compared with the results of empirical and analytical relationships, as well as numerical modeling. Using the results of field measurements of ground settlements and back analysis, the required parameters for predicting the settlement in the next sections have been determined, and it will be possible to predict the settlement in similar future sections with a higher degree of confidence. This finding can provide new strategies for settlement prediction and deformation control methods.

2 Project Specifications

The Mashhad urban train line 2 has a length of 14.3 kilometers, a diameter of 9.4 meters, and a depth of between 10 and 23 meters. The soil layers are often fine-grained (*CL-ML*, USCS classification) up to a depth of 16 meters. From a depth of 16 to 25 meters, it is *SM* and the underground water level is in the depth is 22 meters, almost 3 meters below the lowest level of the tunnel. In Figure 1, the geometric situation of the tunnel placement in the ground layers, the dimensions of the tunnel, the type of the layers' material, and the underground water level are schematically shown [17]. In the first section of the tunnel excavation (northern part), nearly 300 meters long, more than 50 triple rows of settlement pins have been installed and measured. In this research, the settlement that occurred in this part was analyzed and compared with empirical relationships and numerical results.

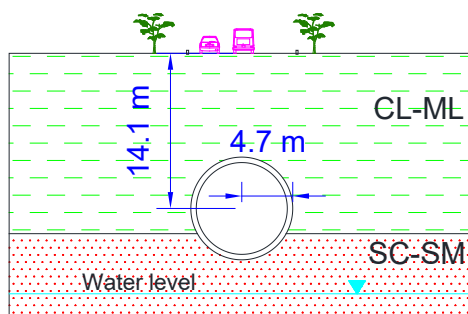


Figure 1

The cross-section of the ground profile and tunnel

3 Surface Ground Settlement Calculation

Reviewing the technical literature on the estimation of surface settlement resulting from tunnel excavation shows various analytical-empirical methods. In these methods, relationships have been presented that estimate the settlement profile at the surface and different depths of the ground. Although these methods are semi-empirical/semi-analytical and give an approximation of deformations, it must be noticed that these methods can be a quick and useful analysis for settlement approximation. In this part, the surface settlement and settlement parameters, including Gaussian curve inflection point, volume loss, and maximum settlement, were calculated using experimental relations and compared with the results obtained from the measured data in the subsequent section.

Peck showed that the ground settlement curve due to tunneling has a normal distribution curve [7]. The settlement profile is increased in depth and has the highest value on the central axis of the tunnel (Gaussian distribution curve) [18]. Based on the data obtained from the measurement of the ground surface settlement profile, the settlement is defined according to the following equation [7, 19].

$$S = S_{max} \times e^{\frac{-x^2}{2i^2}} \quad (1)$$

where S_{max} is the maximum settlement at the vertical tunnel centerline, x is the distance from the axis of the tunnel, i is the curvature point of the settlement curve. The trough width, i , is the distance from the center line of the tunnel to the inflection point of the curve. The total width of the settlement profile is approximately equal to $5i$ [20].

The following empirical equation is also proposed by Attewell to estimate surface settlement [9]:

$$S = (V_s \times e^{\frac{-x^2}{2i^2}}) / \sqrt{2\pi} \quad (2)$$

In equation 2, V_s is equal to the total volume of ground surface settlement in one meter of tunnel length. The volume of the settlement curve per unit of tunnel length (V_s) depends on the type of ground and the drilling method and is obtained from the integration of equation 1 [14]:

$$V_s = \sqrt{2\pi} i S_{max} \quad (3)$$

Another dimensionless parameter called volume loss or ground loss is defined, which is equivalent to the amount of contraction of the tunnel opening. V_L is the surplus volume (in terms of the theoretical volume of the excavated tunnel) of the dug ground and is calculated as the percentage of the volume of the settlement curve (V_s) divided by the volume of the tunnel (V_t) per unit length [14]:

$$V_L = \frac{V_s}{V_t} = \frac{\sqrt{2\pi} i S_{max}}{(\pi D^2 / 4)} \cong 0.319 K \left(\frac{Z_0}{D} \right) \left(\frac{S_{max}}{D} \right) \quad (4)$$

Where Z_0 is the depth of the tunnel axis and D is the diameter of the tunnel. By combining the above equations and considering $i = kZ_0$, the following equation can be deduced, to obtain the S_{max} parameter:

$$S_{max} = \frac{0.313 V_L}{k Z_0} D^2 \quad (5)$$

In order to increase the accuracy of predicting settlements and deformations of the ground caused by tunneling, there is a need to choose the appropriate values of the mentioned parameters. Different methods of obtaining volume loss parameters (V_L), the turning point of the settlement curve (i), and maximum settlement (S_{max}) are given in the following sections.

3.1 Determination of Ground Settlement Measurement Parameters

3.1.1 Inflection Point Parameter (i)

The inflection point of the Gaussian curve, i , has been investigated by many researchers. O'Reilly and New proposed equation 6 to determine the inflection point (i) in a tunnel with a depth of Z_0 [8].

$$\begin{aligned} i &= 0.43Z_0 + 1.1 & 3 < Z_0 < 34 \text{ m} & \text{for cohesion soils} \\ i &= 0.28Z_0 - 0.1 & 6 < Z_0 < 10 \text{ m} & \text{for granular soils} \end{aligned} \quad (6)$$

Other equations presented by other researchers to determine the parameter i are given in Section 6.1.

3.1.2 Volume Loss Parameter (V_L)

In addition to equation 4 which was presented to determine the volume loss, Loganathan and Poulos presented equation 7 to calculate volume loss in shield tunnels [10]. This equation is dependent on the free space parameter (g) and it is obtained from the sum of three components related to the free space behind the tunnel cover resulting from the difference in the diameter of the tunnel cover and trail shield, the three-dimensional shape changes of the working chest and the quality of tunnel excavation.

$$\varepsilon_0 = V_L = \frac{\pi(R + 0.5g)^2 - \pi R^2}{\pi R^2} = \frac{4gR + g^2}{4R^2} \quad (7)$$

where ε_0 and V_L are the volume loss value, R is the radius of the tunnel and g is the gap parameter, and it is obtained according to equation 8.

$$g = G_P + U_{3D}^* + \omega \quad (8)$$

where G_P is the free space outside the lining, U_{3D}^* is equivalent to the three-dimensional elastoplastic deformation of the tunnel face, and ω is a value related to work skill. Due to the use of the EPB tunneling machine and the control of the deformations of the tunnel face, U_{3D}^* is assumed to be equal to zero. Also, the work skill parameter is assumed to be equal to zero. Regarding the injection of grout behind the tunnel lining with cement mortar, G_P is recommended to be assumed equal to 0.07 in the above formula [10].

Table 1 presents the result of volume loss calculations based on equations 7 and 8, taking into account the difference between the boring radius and the outer radius of the tunnel lining (without grout injection, $\omega \cong 0.6G_P$) and the difference between the drilling radius and the lining radius (full injection) and also normal injection (7% space behind the segments).

Table 1
Volume loss calculations based on the Loganathan and Poulos study

Conditions	$V_L(\%)$	$g(\text{m})$	$R(\text{m})$	$D(\text{m})$
No grout injection	3.66	0.17	4.55	9.1
Complete injection	0.18	0.01	4.55	9.1
Normal injection	0.25	0.01	4.55	9.1

3.1.3 Maximum Settlement (S_{\max})

Assuming parameter i is equal to 6.75 meters and considering V_L equal to 0.5, 1, and 2%, the settlement curve is predicted using Peck's equation [7], and depicted in Figure 2.

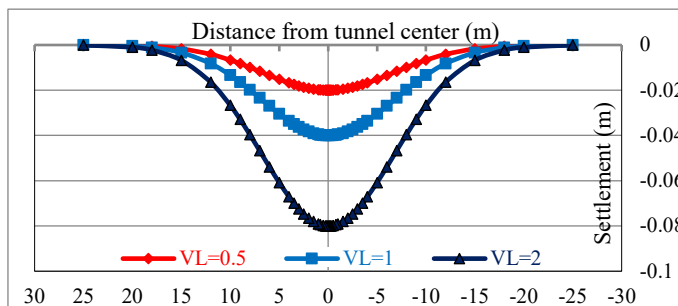


Figure 2
Settlement curve based on Peck's equation

Further, Loganathan and Poulos proposed equation 9 to calculate ground settlement [10].

$$S_{z=0} = 4\varepsilon_0(1-\nu)R^2 \frac{H}{H^2 + y^2} e^{-\frac{1.38y^2}{(H+R)^2}} \quad (9)$$

where ε is the lost volume, ν is Poisson's ratio of the soil above the tunnel, R is the radius of the tunnel, H is the depth of the tunnel, and y is the lateral distance from the tunnel axis. Using the volume loss calculated in section 3.1.2, equal to 0.018 by assuming full injection, and considering the tunnel axis, the maximum settlement is predicted according to Table 2.

Table 2
Prediction of maximum settlement by Loganathan and Poulos's equation

V_L	ν	$R(\text{m})$	$H(\text{m})$	$y(\text{m})$	$S_{z=0}(\text{m})$
0.02	0.35	4.55	14.1	0	0.068

Oteo and Moya also proposed equation 10 to estimate the top settlement of the tunnel (Sarch) [21].

$$S_{arch} = (\psi(0.85-v)\gamma D^2)/E \quad (10)$$

where γ is the density of the earth, D is the diameter of the tunnel, E is Young's modulus of the earth, v is Poisson's ratio, and ψ is a coefficient related to the activation speed of the support inside the tunnel (its values are generally between 0.25 and 0.5, but, for the case when there is no support in the tunnel face, it is equal to one), and S_{arch} is the settlement on the tunnel crest. The values of the maximum ground settlement based on equation 10 are presented in Table 3.

Table 3
Prediction of maximum settlement by Oteo and Moya equation

NO.	ψ	v	$\gamma(\text{kN/m}^3)$	$D(\text{m})$	$E(\text{kN/m}^2)$	$S_{arch}(\text{m})$
1	0.25	0.35	18	9.4	35000	0.006
2	0.5	0.35	18	9.4	35000	0.011

Mair et al. proposed equation 11 to calculate ground settlement [20].

$$(\delta/a) = (s_u/2G)(a/r)e^{(N-1)} \quad (11)$$

where S_u is the undrained shear strength, G is the shear modulus, a is the inner radius of the tunnel, δ is the radial displacement in radius r , and N is the stability ratio ($\sigma_0 = S_u$). Using the above equation, the amount of vertical settlement on the ground surface in two saturated and unsaturated conditions is calculated and presented in Table 4.

Table 4
Prediction of maximum settlement using Mair et al. equation

Conditions	$S_u(\text{kN/m}^2)$	$G(\text{kN/m}^2)$	$a(\text{m})$	$r(\text{m})$	N	δ/a	$\delta(\text{m})$
Saturation	70	13000	4.2	14.1	3.6	0.011	0.045
non-saturated	100	22000	4.2	14.1	2.54	0.003	0.013

Gonzalez and Sagaseta proposed equation 12 relations for soils with cohesion and internal friction angle [22].

$$\varepsilon = \frac{1}{2}\varepsilon_s = \begin{cases} N_c/2I_t & \text{if } N_q < N_{qc} \text{ (elastic)} \\ (N_{cc}/2I_t)[(N_q/N_{qc})^{(1-\sin\phi\sin\theta)}/(\sin\phi(1-\sin\theta))] & \text{if } N_q > N_{qc} \text{ (elastic-plastic)} \end{cases} \quad (12)$$

where in:

$$N_{qc} = \frac{1}{1-\sin\phi}, N_{cc} = \frac{\cos\phi}{1-\sin\phi}, I_r = \frac{G}{(c+p_i\tan\phi)}, N_q = \frac{p_0 + ccot\phi}{p_i + ccot\phi}, N_c = (N_q - 1)cot\phi$$

p_0 is the all-around stress of the earth (vertical and horizontal stress equal), p_i is the tunnel face pressure, c is the cohesion, ϕ is the angle of internal friction, G is the shear modulus, and I_r is the hardness index. Using soil unsaturated parameters, N_{qc} is equal to 0.73 and in the case of applying a working chest pressure of more than 0.73 bar, it should be considered as the elastic state, and in the working face pressure less than 0.7 bar it should be used the elastoplastic relationship. The amount of

ground displacement has been calculated in two cases of tunnel face pressure equivalent to 1.8 bar (average working chest pressure during tunnel excavation) and without applying tunnel face pressure during machine failure and work stoppage (Table 5).

Table 5
Prediction of maximum settlement by Gonzalez and Sagaseta equation

Excavator conditions	Soil conditions	P_0 (kN/m ²)	P_i (kN/m ²)	G (kN/m ²)	C (kN/m ²)	ϕ (°)	v
With working chest pressure	non-saturated	273	180	22000	100	25	–
No chest pressure work	non-saturated	273	0	22000	100	25	0
Excavator conditions	Soil conditions	N_c	N_{ce}	I_r	N_q	N_{qe}	ε (mm)
With working chest pressure	non-saturated	0.51	–	120	1.24	1.73	2
No chest pressure work	non-saturated	2.73	1.57	220	2.27	1.73	7

Chow also presented equation 13 to calculate vertical settlement [23].

$$S = -(\gamma D^2 Z_0^2) / 4G(y^2 + Z_0^2) \quad (13)$$

where γ is the density of the ground, D is the diameter of the tunnel, G is the shear modulus, Z_0 is the depth of the tunnel and y is the distance from the tunnel axis. By using this equation, the settlement curve can be obtained at different distances from the tunnel axis. The maximum settlement on the crest of the tunnel is 18.13 mm according to Chow's relationship.

4 Field Measurement of Settlements

4.1 Observed Ground Surface Settlement

To measure and monitor the deformation of the earth's surface, a leveling method with an accuracy of one millimeter has been used. For this purpose, pins with a depth of about 120 cm in three rows with a longitudinal distance of 10 meters (5 meters in more sensitive sections) and a transverse distance (perpendicular to the path) of 5 meters, before the arrival of the drilling machine, were installed inside the ground and zero reading of their height has been done as a reference point. The position of the surface settlement gauge pins and the tunnel are shown in Figure 3 [24]. To prevent the influence of the surface layer of the earth, the mentioned pins are fastened upon the earth only in their lower 40 cm. In addition to these points,

the surface settlement near the existing structures around the tunnel (distance of 20 meters from the tunnel axis) has also been measured. The settlement recorded at these points was often zero.

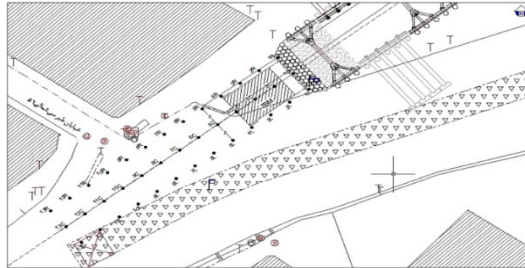


Figure 3

The position of the surface settlement gauge pins (L, C, R), tunnel route axis (a), street (b), residential area (d), and tunnel entrance (e)

All the information used in this paper is the result of reading the above mapping points. The results of the ground surface settlement in the center, left and right sides of the tunnel axis are presented in the diagram of Figure 4. This figure was extracted from [24] report. The settlement of the ground in the center of the tunnel is more than the points on the right and left sides of the tunnel, and the settlement in the points on the left and right sides is almost the same. Also, the settlement of the points, follows virtually the same process.

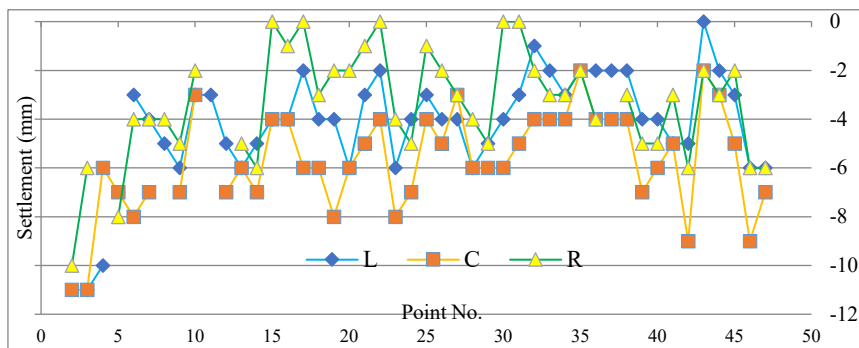


Figure 4

The measured settlement of the ground surface in the center, left, and right sides of the tunnel axis

4.2 Distribution of Settlement in the Longitudinal Section

In shield tunneling, the total ground settlement is caused by the following four stages [25]. Changing the shape of the front and top of the work front due to the release of tension (10 to 20%). This component will be a smaller amount in the case

of machines with the ability to apply pressure to the working face, such as EPB machines. Inductive displacements behind the shield (40 to 50%). These displacements are the result of additional drilling (the difference between the drilling diameter and the diameter of the shield), which is designed to reduce the friction between the shield and the ground, as well as the ease of angling and rotating the shield in curves. Settlement due to the space behind the segments resulting from the difference in the diameter of the tunnel cover and the tail skin (30 to 40%). These displacements can be reduced by grout injecting. Settlement over time caused by tunnel lining deformation and soil creep or consolidation (5 to 10%). The settlement distribution in the longitudinal profile for the excavated path is shown in Figure 5 extracted from [26]. About 12% of the settlement occurred before the arrival of the cutter head, 48% during the excavation, and 40% during the lining and subsequently.

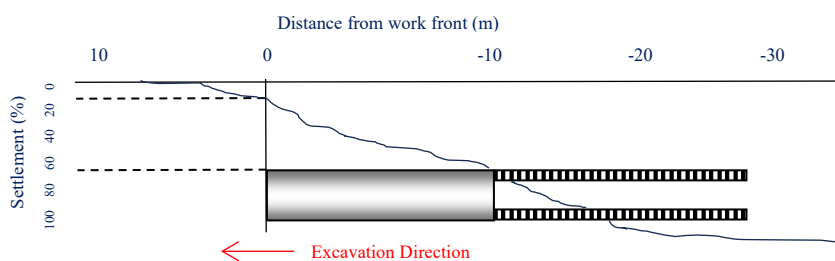


Figure 5

The distribution of the average settlement of the ground surface during tunnel excavation, with an earth pressure balanced shield (EPB)

4.3 The Settlement in the Cross-Section

Due to the presence of three surface settlement control pins, perpendicular to the longitudinal axis, in each row, the approximate transverse profile of the settlement curve can be drawn. The settlement curve of the ground surface for each row of pins is drawn in Figure 6.a, and in Figure 6.b. Further, the average settlement measured in cross-sections, the best adapted Gaussian distribution curve is shown. The ground settlement curve due to the tunnel excavation is in good agreement with the Gaussian curve (Equation 1).

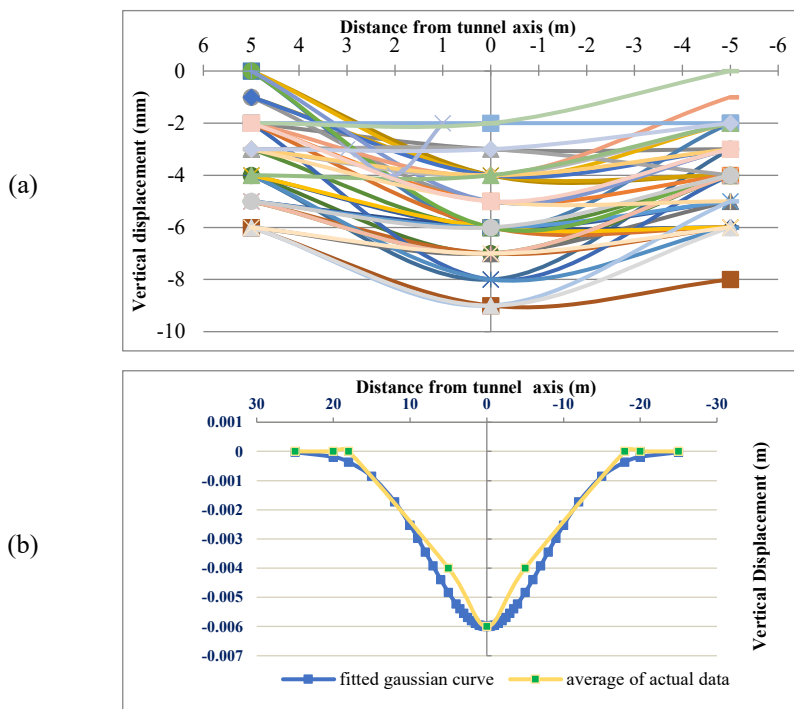


Figure 6

(a) Measured profiles of transverse surface settlement, (b) the average settlement of the ground surface in the cross-section, and the best-fitted Gaussian distribution curve

5 Back Analysis of the Settlement Parameters

Considering that the cross-section of settlements related to tunnel direction can be approximated by the Gaussian distribution curve (Equation 1). It is possible to use the equations related to the Gaussian curve to predict and back analysis of the settlement profile, using data obtained from field measurement. For this purpose, the inflection point of the Gaussian curve (i) can be obtained with the second derivative of equation 1 and the volume loss parameter (V_L) from equation 4. The maximum settlement (S_{max}) using the measured data and the ratio of the inflection point to the tunnel depth, K , are obtained from the equation $K = \frac{i}{z}$. The graphs related to the back analysis of the inflection point parameters of the Gaussian curve (i), volume loss (V_L), maximum settlement (S_{max}), and parameter K obtained by fitting the data with the Gaussian curve (equation 1) are shown in Figure 7. The average of these results is summarized in Table 6.

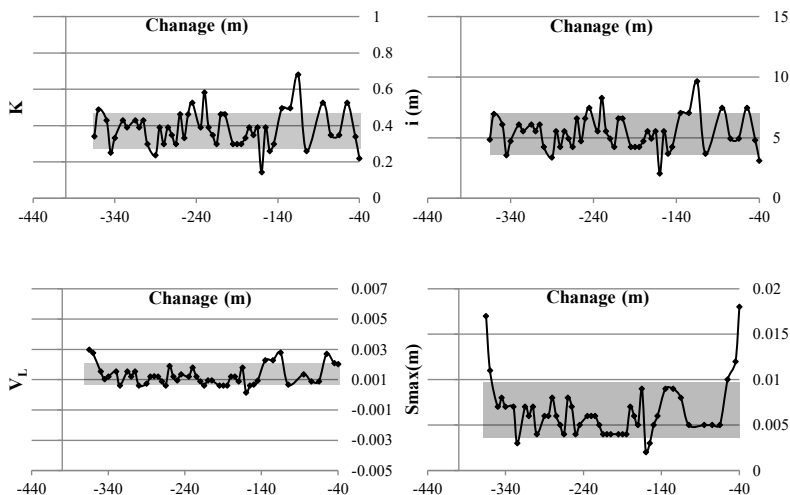


Figure 7

The parameters resulting from the back analysis of the Gaussian surface settlement curve

Table 6

The average results of the back analysis by adopting the Gaussian curve to the measured data

Component	i (m)	K	V_L (%)	S_{max} (mm)
Value	5.4	0.39	0.1	6

6 Comparing the Analytical and Predicted Values

Now, according to the results obtained from the prediction of the various parameters of the settlement curve and compared with the values obtained from the analysis of the measured data, it is possible to predict the settlement of similar sections of the project. The comparison of the measured values of Gaussian curve inflection point parameters, maximum settlement and volume loss parameters with the values obtained from the experimental relations is given in the following sections.

6.1 Gaussian Curve Inflection Point (i)

The presented methods and the calculation values of parameter i , considering the tunnel depth (Z_0) of 14.1 m and the tunnel radius (R) of 4.7 m, based on the suggestions of different researchers are presented in Table 7. The parameter i is calculated by averaging the calculation values, equation 14 [1], whose value is suggested to be equal to 5.75.

$$i_{ave} = \frac{(\sum_{i=1}^n i)}{n} = 5.75 \quad (14)$$

Table 7
Various equations for predicting the inflection point, i

Equation	K	i (m)	Reference
$(i/R) = (Z_0/2R)^n$ ($n = 0.8$ to 1)	-	6.7 ~ 5	Peck (1969) [7]
$i = 0.43Z_0 + 1.1$	-	7.16	O'Reilly and New [8]
$(i/R) = (Z_0/2R)^{0.8}$	-	6.5	Clough & Schmidt [27]
According to the diagram	-	4.8 ~ 7.2	Boscardin and Cording [28]
$i = 0.25(1.5Z_0 + 0.5R)$	-	5.87	Atkinson & Potts [29]
$i = (0.4$ to $0.5)Z_0$	0 ~ 4.5	5.7 ~ 6	Mair & Taylor [20]
$i = 0.5Z_0$	0.5	7	Mair et al. [30]
$(i/R) = (Z_0/2R)^{0.8}$ ($n = 1$)	0.5	7	Attwell & Farmer [31]

According to the different methods for calculating the inflection point of the settlement curve in Table 7, the equations presented by Mair & Taylor (1993) and Atkinson & Potts (1997) have better agreement with the measured values.

6.2 Volume Loss Parameter (V_L)

The volume loss parameter, V_L , is calculated on the basis of the methods provided in Section 3.1.2, and the results are presented in Table 8.

Table 8
Comparison of the volume loss suggested by different researchers with the measured value

Researcher(s)	Proposed V_L (%)	Measured V_L (%)
O'Reilly and New (1982) [8]	1-2	
Mair & Taylor (1993) [20]	1-2	
Mair (2008) [32]	>1	
Lunardi (2008) [33]	0.3	0.1
Loganathan and Poulos (1998) [10]	0.25	
Macklin (1999) [15]	0.4	

According to Table 8, the equations proposed by Lunardi (2008) and Loganathan and Poulos (1998) have a better fit than others.

6.3 Maximum Ground Settlement (S_{max})

The results of calculating the maximum settlement with the methods presented in Section 3.1.3 are also presented in Table 9.

Table 9

Comparison of the maximum sitting suggested by different people with the observed value

Researcher(s)	Proposed S_{max} (mm)	Real S_{max} (mm)
Peck (1969) [7] - $V_L = 0.5\%$	20	
Oteo and Moya (1979) [21]	6	
Mair et al. (1993) [20]	13	6
Gonzalez and Sagaseta (2001) [22]	2	(2 ~ 10)
Loganathan and Poulos (1998) [10]	68	
Chow (1994)	18	

The equations proposed by Oteo and Moya (1979) and Mair et al. (1993) are closer to the average measured values.

7 Numerical Studies

Numerical Finite Element (FE) modeling is a useful tool for simulation and prediction of ground-induced deformation by tunneling. Using numerical methods, it is possible to calculate the distribution of stress and strain in the ground adjacent to the tunnel space due to the complex interaction between excavation and tunnel construction methods and the initial stress distribution, which often indicates inhomogeneous behavior. It is also possible to effectively consider the non-linear behavior depending on time or multi-stage construction.

7.1 Numerical Modeling

A numerical analysis of the tunnel construction was conducted to compare the measured tunneling-induced settlements with the calculated deformation of numerical modeling. According to geotechnical studies, the earth's materials are often lean clay with silt and silty sand. The input parameters to the model for the specifications of the equivalent soil layers and tunnel lining parameters are presented in Tables 10 and 11. A traffic and surcharge load is also equal to $20 \frac{\text{kN}}{\text{m}^2}$ as a distributed load applied in the model.

Table 10

Engineering parameters of soil layers

Layer depth (m)	Soil	γ_d (kN/m ³)	Moisture (%)	Cohesion (kN/m ²)	Internal friction	Elasticity modulus (kN/m ²)	ν	Undrained shear strength
0 ~ 16	CL-ML	15.5	20	35	25°	36000	0.35	100 kN/m ²
16 ~ 25	SM	19	27	1	35°	64000	0.33	-

Table 11
Specifications of the concrete segment of the tunnel lining

Description	E (kN/m ²)	EA (kN/m)	EI (kNm ² /m)	ν	W (kN/m/m)
Concrete cover (segment)	35000000	12250000	125000	0.15	8.4

In this study, two-dimensional Plaxis software was used. Among the advantages of the mentioned software is the possibility of multi-stage construction and the use of various constitutive models [34]. The boundaries of the model in the horizontal direction from the center of the tunnel are considered to be five times the radius of the tunnel and in the vertical direction, two and a half times the radius of the tunnel. Deformation outside this range can be ignored. For the meshing of the model, the 15-node element was used as the basic element type, and according to the concentration of stress around the tunnel, the mesh was refined in these areas. Considering that during the two phases of digging and tunnel construction, the soil around the tunnel is loaded and the hardening soil model differentiates between pristine loading and loading-reloading, this behavior model can be used for tunnel modeling [35, 36]. Staged construction analysis is done according to the existing stresses, maintenance of the tunnel face during drilling with a shield, installation of the final segment, injection of the space behind the lining, and contraction to the tunnel cover. The initial stage is to model the initial equilibrium, and after the model reaches the equilibrium, the settlement becomes zero. The settlement in the next stages is measured relative to the initial stage. In the second stage, the tunnel is modeled by the machine, and the tunnel is uncovered. At this stage, the drilling machine has endured some load and $\sum Mstage$ can be considered to be about 0.5 [35]. In the next step, the installation of the tunnel lining is modeled. The injection behind the segments can be modeled by applying a large load equivalent to the injection pressure (between 1.5 and 2 bar in the present study). The reduced volume is caused by the deformation of the tunnel lining, additional soil excavation (space behind the tunnel lining), and water drainage. In this study, the value of volume loss (V_L) was determined based on the real data obtained from the surface settlement control ($V_L = 0.1\%$) and applied in the numerical model.

7.2 Results

Calculation of the settlement with the numerical model shows that the maximum vertical settlement of the tunnel on the tunnel centerline and corresponding to the tunnel crest is equal to 9 mm and the settlement of the ground surface is 6 mm. The settlement curves of the ground are presented in Figure 8.

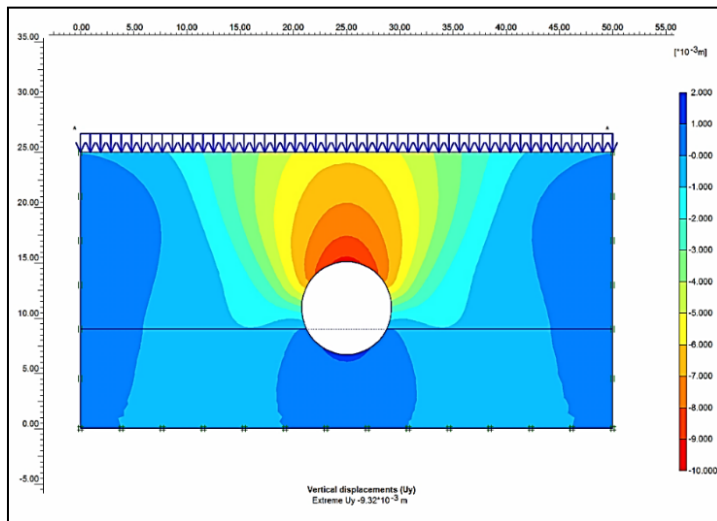


Figure 8
Curves of vertical settlement of the soil mass

The ground surface settlement curve above the tunnel axis is close to the average real measured deformations, next to the fitted Gaussian curve to the measured data, and the curve resulting from the numerical models, are presented in Figure 9. The broader curve from the numerical model is a little wider than the Gaussian curve, that is, in this case, the trough width or distance from the center line of the tunnel to the inflection point of the curve (i) is greater. Although the total width of the settlement profile is often considered to be approximately equal to $5i$, in this study the total width of the settlement profile is about $6i$ for numerical studies and about $6.5i$ for the experimental equations and measured values.

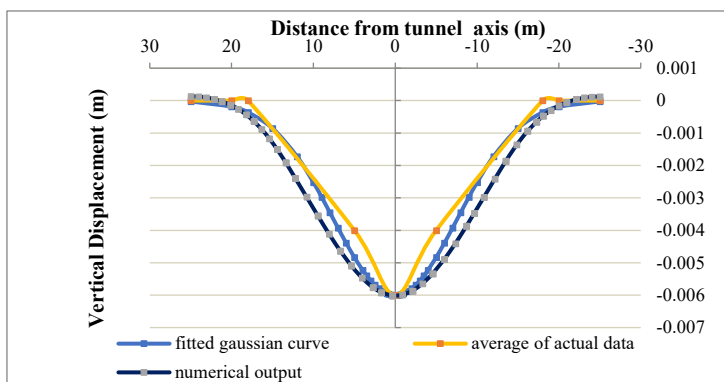


Figure 9
Surface settlement curve obtained from measured values, results of the numerical model, and Gaussian distribution curve

Conclusions

Among the many existing methods, through detailed comparison with the measured values, the most appropriate experimental and analytical relationships have been identified, for the prediction of the settlement parameters S_{\max} , i , V_L , etc. of the ground. The conclusions can be summarized as follows:

- The average maximum surface settlement that usually occurs on the ground above the tunnel centerline is equal to 6 mm.
- The average horizontal distance of the turning point of the settlement curve with the axis of the tunnel (parameter i) is estimated to be about 5.4 meters. Therefore, the settlements of the tunnel in the transverse direction become insignificant at a distance of 15 meters (equivalent to $3i$) and the structures outside it can be assumed to be safe.
- The average volume loss parameter (V_L) has been calculated to be about 0.1% of the tunnel volume, which is less than the usual world experiences for soft ground.
- The back analysis with the numerical model shows that the trough width of the settlement curve obtained from the numerical studies is about 1 meter (20%) larger than the experimental curve (Gaussian curve fitted to the real data).
- By using the calibrated numerical model, it is possible to more accurately predict ground subsidence.

Acknowledgment

This research was partially funded by the 2020-1.1.2-PIACI-KFI-2020-00129 project.

References

- [1] Chakeri, H., Y. Ozcelik, and B. Unver, *Effects of important factors on surface settlement prediction for metro tunnel excavated by EPB*. Tunnelling and Underground Space Technology, 2013. **36**: p. 14-23
- [2] Kazemian, M., et al., *Effects of Wheel Surface Defects on Ground Borne Vibration*. Acta Polytech. Hung, 2022. **19**: p. 129-141
- [3] Fischer, S., *Geogrid reinforcement of ballasted railway superstructure for stabilization of the railway track geometry—A case study*. Geotextiles and geomembranes, 2022. **50**(5): p. 1036-1051
- [4] Jóvér, V., et al., *Investigation of the Geometrical Deterioration of Paved Superstructure Tramway Tracks in Budapest (Hungary)*. Infrastructures, 2023. **8**(8): p. 126
- [5] Jóvér, V., et al., *Investigation of “Open” Superstructure Tramway Tracks in Budapest*. Infrastructures, 2023. **8**(2): p. 33

-
- [6] Fischer, S. and S.K. Szürke, *Detection process of energy loss in electric railway vehicles*. Facta Universitatis, Series: Mechanical Engineering, 2023. **21**(1): p. 081-099
- [7] Peck, R.B., *Deep excavations and tunneling in soft ground*. Proc. 7th ICSMFE, 1969, 1969: p. 225-290
- [8] O'REILLY, M.P. and B. New, *Settlements above tunnels in the United Kingdom-their magnitude and prediction*. 1982
- [9] Attewell, P., *Predicting the dynamics of ground settlement and its derivatives caused by tunnelling in soil*. Ground engineering, 1982. **15**(8): p. 13-22
- [10] Loganathan, N. and H. Poulos, *Analytical prediction for tunneling-induced ground movements in clays*. Journal of Geotechnical and geoenvironmental engineering, 1998. **124**(9): p. 846-856
- [11] Chou, W.-I. and A. Bobet, *Predictions of ground deformations in shallow tunnels in clay*. Tunnelling and underground space technology, 2002. **17**(1): p. 3-19
- [12] Pinto, F. and A.J. Whittle, *Ground movements due to shallow tunnels in soft ground. I: analytical solutions*. 2014
- [13] McCabe, B., et al., *Settlement trough parameters for tunnels in Irish glacial tills*. Tunnelling and underground space technology, 2012. **27**(1): p. 1-12
- [14] Wang, Z., et al., *Finite element analysis of long-term surface settlement above a shallow tunnel in soft ground*. Tunnelling and underground space technology, 2012. **30**: p. 85-92
- [15] Macklin, S., *The prediction of volume loss due to tunnelling in overconsolidated clay based on heading geometry and stability number*. Ground engineering, 1999. **32**(4): p. 30-33
- [16] Jiang, M. and Z.-Y. Yin, *Influence of soil conditioning on ground deformation during longitudinal tunneling*. Comptes Rendus Mecanique, 2014. **342**(3): p. 189-197
- [17] Mir Mehrabi, h.a.M., M. A., *Prediction and investigation of settlement caused by tunnel excavation by numerical method and comparison with measured values (In Persian)*, in *The 2nd Iran Dam and Tunnel Conference*. 2013: Tehran, Iran
- [18] Ter-Martirosyan, A.Z., et al., *Surface Settlement during Tunneling: Field Observation Analysis*. Applied Sciences, 2022. **12**(19): p. 9963
- [19] Ding, Z., et al., *Theoretical analysis on the deformation of existing tunnel caused by under-crossing of large-diameter slurry shield considering construction factors*. Tunnelling and Underground Space Technology, 2023. **133**: p. 104913

- [20] Mair, R., R. Taylor, and A. Bracegirdle, *Subsurface settlement profiles above tunnels in clays*. Geotechnique, 1993. **43**(2): p. 315-320
- [21] Oteo, C. and J. Moya. *Evaluación de parámetros del suelo de Madrid con relación a la construcción de túneles*. in *Proceedings of the 7th European Conference on Soil Mechanics and Foundation Engineering, Brighton*. 1979
- [22] González, C. and C. Sagaseta, *Patterns of soil deformations around tunnels. Application to the extension of Madrid Metro*. Computers and Geotechnics, 2001. **28**(6-7): p. 445-468
- [23] Chow, L., *The prediction of surface settlements due to tunnelling in soft ground*. M. Sc, 1994
- [24] Organization, M.S.L.T., *Analysis of Ground Settlements between North Shaft and Station A2 (in Persian)*. 2012
- [25] Leca, E. and B. New, *Settlements induced by tunneling in soft ground*. Tunnelling and Underground Space Technology, 2007. **22**(2): p. 119-149
- [26] Mirmehrabi, H., Maroof, A., *Prediction of surface subsidence of Mashhad city train line 2 tunnel: analytical methods and comparing with monitoring results (in Persian)*. Retrofit. Rehabil. Ind., 2014. **11**: p. 30-39
- [27] Clough, G.W. and B. Schmidt, *Design and performance of excavations and tunnels in soft clay*. 1981
- [28] Boscardin, M.D. and E.J. Cording, *Building response to excavation-induced settlement*. Journal of Geotechnical Engineering, 1989. **115**(1): p. 1-21
- [29] Atkinson, J. and D. Potts, *Subsidence above shallow circular tunnels in soft ground*. Journal of the Geotechnical Engineering Division, 1977. **103**(4)
- [30] Mair, R., M. Gunn, and M. O'reilly, *Ground movement around shallow tunnels in soft clay*. Tunnels & Tunnelling International, 1982. **14**(5)
- [31] Attewell, P. and I. Farmer, *Ground deformations resulting from shield tunnelling in London Clay*. Canadian Geotechnical Journal, 1974. **11**(3): p. 380-395
- [32] Mair, R. *Research on tunnelling-induced ground movements and their effects on buildings—lessons from the Jubilee Line Extension. Keynote Lecture*. in *Proceedings of International Conference on Response of Buildings to Excavation-induced Ground Movements, held at Imperial College, London, UK*. 2001
- [33] Lunardi, P., *Design and construction of tunnels: Analysis of Controlled Deformations in Rock and Soils (ADECO-RS)*. 2008: Springer Science & Business Media
- [34] Mohammadzadeh, D., et al. *Urban train soil-structure interaction modeling and analysis*. in *Engineering for Sustainable Future: Selected papers of the*

18th International Conference on Global Research and Education Inter-Academia–2019 18. 2020. Springer

- [35] Brinkgreve, R., et al., *2D–Version 8*. Delft, Delft University of Tehnology & PLAXIS bv, 2004. **18**
- [36] Mohammadzadeh, D., et al., *Three-Dimensional Modeling and Analysis of Mechanized Excavation for Tunnel Boring Machines*. Acta Polytech. Hung, 2021. **18**: p. 213-230